

The influence of 2 kbar pressure on the global and internal dynamics of human hemoglobin observed by quasielastic neutron scattering

Marie-Sousai Appavou · Sebastian Busch ·
Wolfgang Doster · Ana Gaspar · Tobias Unruh

Received: 30 June 2010 / Revised: 12 January 2011 / Accepted: 25 January 2011 / Published online: 22 February 2011
© European Biophysical Societies' Association 2011

Abstract Pressure is a ubiquitous physical parameter in life and is commonly used in the life sciences to study new protein folding pathways or association-dissociation phenomena. In this paper, an investigation of the influence of pressure on hemoglobin, a multimeric protein, at the picosecond time scale is presented using time-of-flight neutron scattering. The aim is to observe the influence of pressure on the translational diffusion and internal motions of hemoglobin in a concentrated solution and a possible dissociation of the subunits as suggested by Pin et al. (Biochemistry 29:9194, 1990) using fluorescence spectroscopy. A new flat 2 kbar pressure cell made of an aluminum alloy has been used, which allowed the effect of pressure to be studied with minimum background contribution. Within this range of pressure, the effect of this physical parameter on global diffusion can be explained in terms of the change in the water buffer viscosity and an oligomerization of hemoglobin subunits, whereas the internal motions were less affected.

Keywords Pressure · Protein · Hemoglobin · Dynamics · Quasielastic neutron scattering

M.-S. Appavou (✉)
Forschungszentrum Jülich GmbH, Institute for Solid State Research, Jülich Center for Neutron Science at FRM II, Lichtenbergstraße 1, 85747 Garching bei München, Germany
e-mail: m.s.appavou@fz-juelich.de

M.-S. Appavou · S. Busch · W. Doster · A. Gaspar · T. Unruh
Physik Department E13, Technische Universität München, James Franck Straße 1, 85747 Garching bei München, Germany

S. Busch · A. Gaspar · T. Unruh
Forschungsneutronenquelle Heinz Maier-Leibnitz (FRM II), Technische Universität München, Lichtenbergstraße 1, 85747 Garching bei München, Germany

Introduction

Pressure is a physical parameter that is omni-present on earth. Indeed, micro-organisms such as *Bacillus licheniformis* can live in the deep seas up to a depth of 10 km, where they sustain a pressure of about 1 kbar (Masson et al 2001; Feijoo et al. 1997). Moreover, pressure is being used more and more in sterilization and bioconservation processes in food and pharmaceutical industries.

Pressure has stabilizing and destabilizing effects on proteins. The destabilizing effect is essentially due to compression-induced electrostriction in electrostatic interactions and reorganized water molecules, which are important in the framework of the hydrophobic interactions. The stabilizing effect of pressure is induced by the decrease in distances, essentially through the influence on van der Waals interactions and hydrogen bonds. A combination of pressure and temperature leads to a reentrant phase diagram describing an ellipse delimiting thermal and pressure conditions for the protein to be in the native state. In general, the dissociation of oligomeric proteins and large scale structures is observed at atmospheric pressures up to 2 kbar and the unfolding of monomeric proteins from 3 to 8 kbar. Several reviews edited by Balny, Masson, and Heremans in *Biochimica et Biophysica Acta* in 2002 show the large panel of studies undertaken using several techniques and on several proteins (Balny et al. 2002).

Quasielastic neutron scattering allows internal motions of proteins to be explored at the Ångström scale on the picosecond time scale (McCammon and Harvey 1988; Bée 1988). Few neutron-scattering studies on biomolecules have been performed using this physical parameter up to date. The first unfolding study using inelastic neutron scattering was published by Doster and Gebhardt (2003)

and Doster et al. (2003). Other recent studies have been performed by Appavou et al. for BPTI (Appavou et al. 2006) and by Di Bari et al. (2000) for trypsin. In the following, a series of results on human hemoglobin is presented as a function of pressure, obtained using the time-of-flight neutron-scattering spectrometer TOFTOF at FRM II (Garching bei München, Germany).

A pressure cell has been built that can sustain a pressure of 2 kbar. The high transmission, due to the aluminum alloy AL7075 of the cell, allows the influence of pressure on the translational diffusion and the internal dynamics of hemoglobin to be observed.

Hemoglobin is a tetrameric protein with a molecular weight of about 62 kDa, composed of 574 amino acid residues. Each subunit—the $\alpha 1$, $\alpha 2$, $\beta 1$, and $\beta 2$ chains—has a structure that is similar to another model protein, myoglobin. Hemoglobin proteins are enclosed in red blood cells where the concentration can reach 330 mg/ml under physiological conditions. Its role is to bring the oxygen molecules from the lung to the other cells in the organism.

Previous studies were performed in particular about the concentration dependence of the association-dissociation constant of the subunits (Edelstein et al. 1970; Philo et al. 1988). It has been shown that at low concentration, hemoglobin is a dimer, whereas at higher concentration, it is a tetramer. A high pressure experiment has already been performed on this protein using fluorescence spectroscopy (Pin et al. 1990). The authors have found a dissociation from dimer to monomer around 1 kbar for a 10^{-6} M concentration of hemoglobin in solution and a dissociation from tetramer to dimer for a 10^{-5} M concentration. In the following, results of small-angle neutron scattering are also reported that were performed with the aim of determining the association state of this system at atmospheric pressure in the very concentrated aqueous solution used for the time-of-flight experiments.

Materials and methods

Hemoglobin solution preparation

The sample was a concentrated hemoglobin solution at 320 mg/ml in deuterated phosphate buffer with pD 6.08. Human hemoglobin powder was purchased from Sigma-Aldrich (H7379). The powder was dissolved in a phosphate buffer prepared in D_2O by mixing a solution of NaD_2PO_4 in D_2O with a solution of Na_2DPO_4 in D_2O . The phosphate salts were H/D exchanged by dissolution in D_2O and dried over silica gel beforehand. The $pD = pH + 0.4$ was adjusted by adding a few microliters of either NaD_2PO_4/D_2O or Na_2DPO_4/D_2O solutions.

Neutron measurements

The TOFTOF time-of-flight spectrometer at FRM II (Unruh et al. 2007, 2008) was used to study the quasielastic broadening as a function of pressure from atmospheric pressure up to 2 kbar. The following configuration of the spectrometer was chosen: wavelength $\lambda = 6.0 \text{ \AA}$, chopper speed = 12,000 rpm, and frame overlap ratio 4. This made it possible to access the 20 ps time scale to investigate the internal motions of the protein (Gaspar 2007). In order to further increase the signal-to-noise ratio during acquisition, the sample chamber was filled with argon gas.

We studied the influence of pressure from atmospheric pressure up to 2 kbar at 300 K (27°C). The temperature was controlled with a thermo-bath containing silicon oil and checked with a thermocouple sensor.

ANTARES at FRM II is an instrument for neutron radiography and tomography (Schillinger et al. 2006) and was used in order to see whether the high pressure cell was completely filled with the sample solution during the quasielastic neutron-scattering measurements. The neutron flux for this setting was $2.5 \times 10^7 \text{ neutrons s}^{-1} \text{ cm}^{-2}$. The exposure time for a single radiograph was 40 s, the field of view about $226 \times 226 \text{ mm}$.

Finally, the small-angle neutron-scattering configuration of the instrument MIRA at FRM II (Georgii et al. 2007) was used to determine the association state of hemoglobin in the solution at atmospheric pressure. The wavelength was $\lambda = 9.27 \text{ \AA}$ in order to access a space at scales up to 0.35 \AA^{-1} . The hemoglobin solution and the deuterated phosphate buffer were put into a Hellma quartz cell with 1 mm thickness. Data were treated with the program GRASP from the Institut Laue-Langevin (Grenoble, France) (Dewhurst 2001). The aggregation state of hemoglobin in the solution was determined to be tetrameric at atmospheric pressure.

Experimental 2 kbar pressure set-up

A new flat 2 kbar pressure cell was made in an aluminum alloy (Al7075, approx. $AlZn_6Mg_3Cu_2$) obtained from Alimex (Willich, Germany) and was used in order to reduce the contribution from the sample holder. The 2 kbar pressure cell has a flat shape (5 mm thickness) in which 10 parallel channels with a diameter of $d = 1.6 \text{ mm}$ each contain the sample (Fig. 1). The surfaces of the channels have a distance of at least d from the surface of the cell and $2d$ from the ones of the neighboring channels.

The transmission of the cell at a neutron wavelength of $\lambda = 6 \text{ \AA}$ when oriented perpendicular to the neutron beam was calculated as 96.6%. It should be noted that the absorption of the aluminum alloy has a far stronger influence on the transmission values than the scattering. When

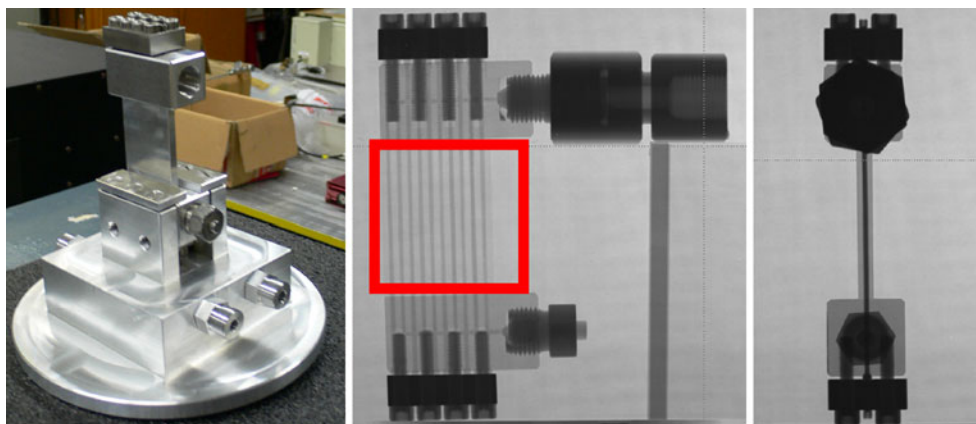


Fig. 1 *Left* The 2 kbar pressure cell. *Middle* and *right* Neutron radiography pictures of the 2 kbar pressure cell from ANTARES. The *square* represents the sample area for the TOFTOF experiments

filled with buffer, the transmission was calculated as 91.8% and with the protein solution (320 mg/ml) 86.2%.

The cell is filled using a syringe, and a membrane is used in an adaptor to separate the sample from the liquid transmitting the pressure from the spindle. Figure 1 presents some pictures from neutron radiography measurements on ANTARES showing that the cell was completely filled during the experiment. We used D₂O as a liquid to transmit the pressure through a capillary connected to the cell with the adaptor on one side and to the spindle containing the liquid in a syringe on the other side. A pressure gauge continuously indicated the pressure inside the system. Figure 2 gives a description of the set-up of the instrument.

The presented set up was used for the investigation of the influence of pressure from atmospheric pressure up to 2 kbar at 300 K (27°C). This temperature was chosen in order to check that our data were consistent with data acquired at atmospheric pressure and similar systems but in a classical aluminum sample holder (Gaspar et al. 2008), which was the case. The temperature was controlled by a thermo-bath containing silicon oil and checked with a thermocouple sensor glued to the cell with aluminum tape as close as possible to the sample area.

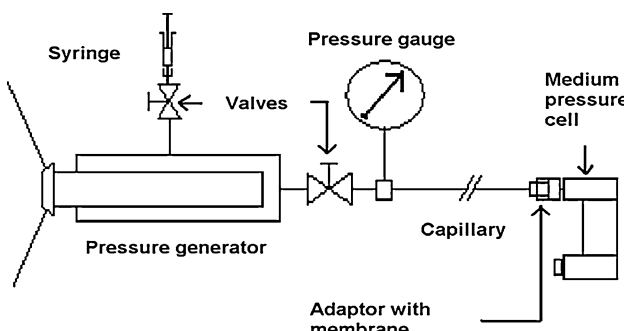


Fig. 2 Schematic of the 2 kbar pressure set up

The measurement time for each pressure point was 10 h. Each pressure point (1 and 2 kbar) was reached carefully by increasing the pressure slowly (0.2 kbar/min) with pauses made each 0.5 kbar for 5 min. Measurements started after reaching the right temperature.

Data treatment and analysis

The data reduction and analysis were performed using the program FRIDA (<http://iffwww.iff.kfa-juelich.de/~wuttke/doku/doku.php?id=frida:frida>). The measured time-of-flight spectra were normalized to the monitor and to the vanadium flat plate standard (1.1 mm thickness), converted to energy transfer and from $\partial\sigma/\partial\omega\partial2\theta$ to the dynamic structure factor $S(2\theta, \omega)$ and corrected for differences in detector efficiency for neutrons of different final energies.

A self-absorption correction procedure was performed using FRIDA. The sample volume was approximated as a flat slab with the same content as the actual cylinders (correspondingly with a thickness of 0.63 mm), which made an analytical calculation of the self absorption correction coefficients possible (see e.g., Bée 1988).

For the structural investigation, static structure factors were obtained integrating the two-dimensional spectra over the energy transfer:

$$S(2\theta) = \int_{-E_i}^{+\infty} S(2\theta, \omega) d\omega \quad (1)$$

and subsequently transforming 2θ to the wave vector q via $q = (4\pi/\lambda) \cdot \sin \theta$.

For the dynamic investigation, the spectra were regrouped into slices of constant q and the incoherent dynamic structure factor $S_{\text{inc}}(q, \omega)$ was evaluated. It is the space-time Fourier transform of the self-correlation of the

position of an atom at time 0 with the position of the same atom at time t :

$$S_{\text{inc}}(\vec{q}, \omega) = \sum_i \frac{1}{N2\pi} \int_{-\infty}^{+\infty} e^{-i\omega t} \left\langle e^{i\vec{q} \cdot \vec{r}_i(t)} e^{-i\vec{q} \cdot \vec{r}_i(0)} \right\rangle dt \quad (2)$$

The D₂O buffer spectra were subtracted from the protein solution using the equation:

$$S(q, \omega)_{\text{protein}} = S(q, \omega)_{\text{protein solution}} - \varphi_{\text{buffer}} \cdot S(q, \omega)_{\text{buffer}} \quad (3)$$

where φ_{buffer} is the volume fraction of buffer. It was calculated such that it does not include the first hydration shell of the protein because these molecules are known to have significantly different properties from the bulk (see e.g., Perez et al. 1999).

In order to enhance and easily discriminate the signal coming from the slow global translational diffusion located in the quasielastic component from the one related to the fast internal as well as the high frequency vibrational motions, the dynamic susceptibility $\chi''(q, \omega)$ was calculated from the dynamic structure factor using (Wuttke et al. 2000):

$$\chi''(q, \omega) = \frac{S(q, \omega)}{n(q, \omega)} \quad (4)$$

where $n(q, \omega)$ is the Bose factor that was used in its first-order approximation:

$$n(q, \omega) = \frac{1}{\exp\left(\frac{\hbar\omega}{k_B T}\right) - 1} \approx \frac{k_B T}{\hbar\omega}. \quad (5)$$

D₂O buffer dynamics analysis

The D₂O buffer spectra from which the empty can had been subtracted and the absorption corrected were fitted with a single Lorentzian:

$$L_{\text{dif,int}}(q, \omega) = \frac{\Gamma_{\text{dif,int}}}{\Gamma_{\text{dif,int}}^2 + \omega^2}. \quad (6)$$

The extracted line width Γ was plotted as a function of the square of the wave vector and fitted with a jump model, which is the normal model for water diffusion (Bée 1988):

$$\Gamma(q^2) = \frac{Dq^2}{Dq^2\tau_0 + 1}, \quad (7)$$

where D is the self-diffusion coefficient of the water molecules and τ_0 the residence time.

Moreover, a simple long-range diffusion model was used to fit the line width Γ according to:

$$\Gamma(q^2) = Dq^2. \quad (8)$$

Hemoglobin dynamics analysis

After absorption correction, empty can subtraction, and D₂O spectra subtraction, the protein dynamic structure factors were fitted:

$$S(q, \omega)_{\text{protein}} = P(q) \cdot \{ L_{\text{dif}}(q, \omega) \otimes [A_0 \cdot \delta(\omega) + (1 - A_0) \cdot L_{\text{int}}(q, \omega) + B(q)] \} \otimes S_{\text{res}}(q, \omega) \quad (9)$$

where $P(q)$ is the form factor including coherent contributions of the protein scattering (the elastic form factor) and vibrational motions expressed by the Debye-Waller factor. \otimes denotes the convolution in ω -space. L_{dif} is a Lorentzian that accounts for the global diffusion of the protein in the solution (cf. Eq. 6). The q -dependence of its line width is evaluated in the low- q limit (below 1 Å⁻¹) as $\Gamma = D_{\text{app}}Q^2$ where D_{app} is the apparent self-diffusion coefficient of the protein, L_{int} is the Lorentzian that accounts for internal motions, and A_0 is the elastic incoherent structure factor (EISF), which gives information about the internal motions and the fraction of immobile nonexchangeable protons involved in internal motions. For a particle moving in a harmonic potential, the EISF is a Gaussian:

$$A_0(q) = p + (1 - p) \cdot \exp[-q^2 \langle \Delta x^2 \rangle] \quad (10)$$

where $\langle \Delta x^2 \rangle$ is the mean square displacement, P is the fraction of immobile nonexchangeable protons, $B(q)$ is a background factor caused by the low frequency vibrations overlapping the quasielastic line, and $S_{\text{res}}(q, \omega)$ is the resolution function of the instrument obtained by the measurement of a flat plate of vanadium.

Results and discussion

Performance of the 2 kbar pressure cell in neutron experiments

Figure 3 displays the contributions of the new pressure cell, the buffer, and of the protein to the signal detected at the instrument TOFTOF. As can be seen, the contribution of the cell is smaller than that of the sample. This first result shows that this pressure cell is particularly appropriate for neutron scattering.

Analysis of the D₂O buffer dynamics

The dynamic susceptibilities at different q values for the D₂O buffer at atmospheric pressure are plotted in Fig. 4.

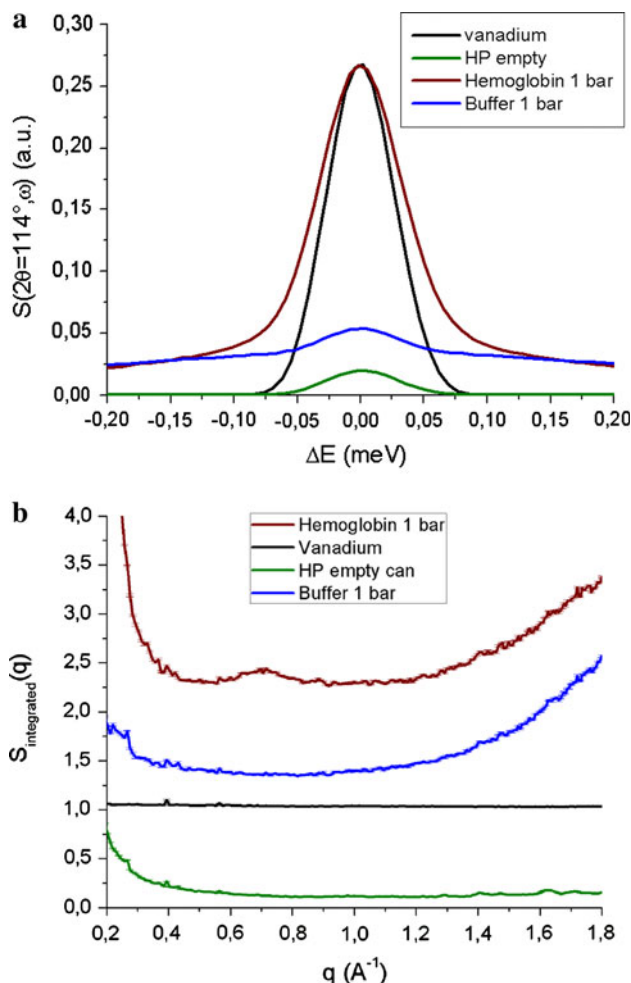


Fig. 3 **a** The dynamic structure factor $S(2\theta = 114^\circ, \omega)$ for the empty cell, the buffer solution in the cell, the protein solution in the cell, and the vanadium reference for comparison. The signal caused by the cell is lower than the contribution of the buffer and much lower than that of the hemoglobin solution. **b** The structure factor corresponding to the energy-integrated intensity of $S(2\theta, \omega)$ for the empty cell, the buffer solution, the protein solution, and the vanadium reference for comparison at atmospheric pressure. Again, the cell contribution is lower than that of the buffer and much lower than that of the hemoglobin solution

A shift of the peak frequency as a function of q can be seen that is characteristic for the heavy water global diffusion (Cavatorta et al. 1994; Longeville and Lechner 2000). The dynamic susceptibilities at low and high q values for the D_2O buffer at different pressure are plotted in Fig. 5.

In Fig. 5, the arrows emphasize the changes in the intensities with increasing pressure and, at low q , the shift to lower frequencies due to the decrease in the water global dynamics. At high q , the decrease in the intensities with increasing pressure and the shift to higher frequencies is visible. This is probably partially due to the shift of the characteristic peak of D_2O in the structure factor around

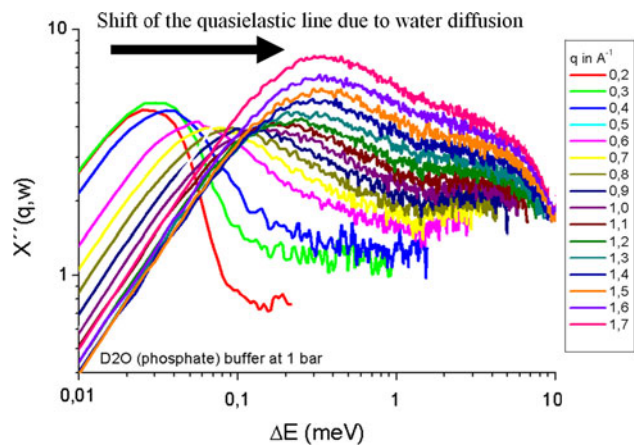


Fig. 4 q Dependence of the dynamic susceptibility for the D_2O buffer at atmospheric pressure

2 \AA^{-1} (Doster et al. 2003) and also to the hydrogen-bond rearrangement (already seen by NMR) (Prielmeier et al. 1987).

The dynamic structure factor of the D_2O buffer was fitted with a single Lorentzian. The line width is plotted as a function of the square of the wave vector in Figs. 6, 7. The line width has been fitted with a jump model (cf. Eq. 7) and a long-range diffusion model (cf. Eq. 8).

The values obtained by using the jump model for the translational diffusion coefficient ($2.34 \times 10^{-5} \text{ cm}^2/\text{s}$) and the residence time $\tau = 0.7 \text{ ps}$ are close to those obtained by Chen et al. (1982). By using the simple long-range diffusion model, we have obtained a translational diffusion coefficient of $1.76 \times 10^{-5} \text{ cm}^2/\text{s}$.

The analog curves for 1 and 2 kbar are presented in Fig. 7.

An increase in the D_2O diffusion is observed when increasing pressure to 1 kbar ($2.45 \times 10^{-5} \text{ cm}^2/\text{s}$ with the jump model and $1.81 \times 10^{-5} \text{ cm}^2/\text{s}$ with the long-range diffusion model) and then a lowering ($2.12 \times 10^{-5} \text{ cm}^2/\text{s}$ with the jump model and $1.76 \times 10^{-5} \text{ cm}^2/\text{s}$ with the long-range diffusion model) at 2 kbar, which is in agreement with the behavior of the heavy water viscosity under pressure (Bett and Cappi 1965). The residence time seems to decrease with increasing pressure, which might be due to de Gennes narrowing: the structure factor maximum of D_2O shifts with increasing pressure to higher q values as the intermolecular distance is shorter than at atmospheric pressure as well as at 1 kbar. Therefore, the narrowing of the half width at half maximum occurs at higher values of q , which leads to an apparent shorter residence time. A similar effect of shortening residence times was however also found in H_2O where de Gennes narrowing has no disturbing effect (Longeville and Lechner 2000; Cunsolo et al. 2006).

Fig. 5 Dynamic susceptibilities at $q = 0.6 \text{ \AA}^{-1}$ (left) and at $q = 1.8 \text{ \AA}^{-1}$ (right) for the D₂O buffer at atmospheric pressure (red line), at 1 kbar (green line), and at 2 kbar (blue line)

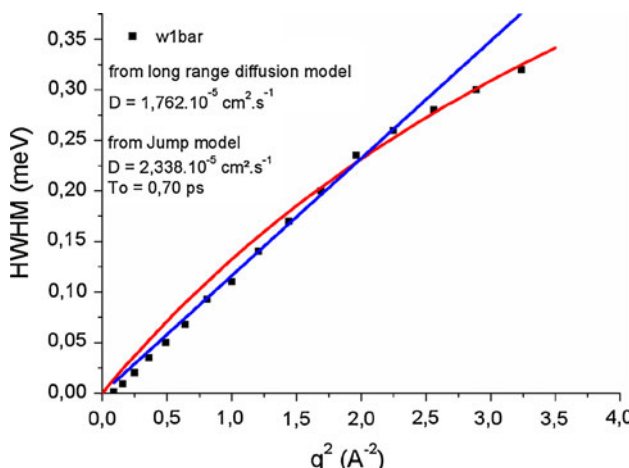
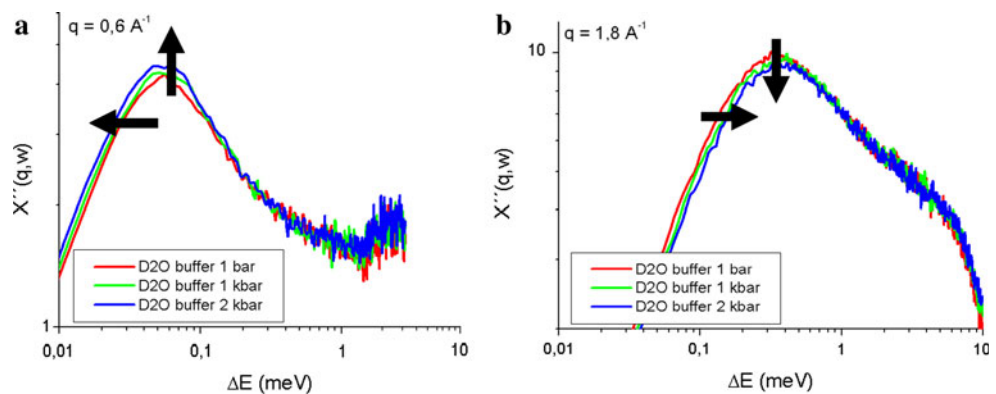
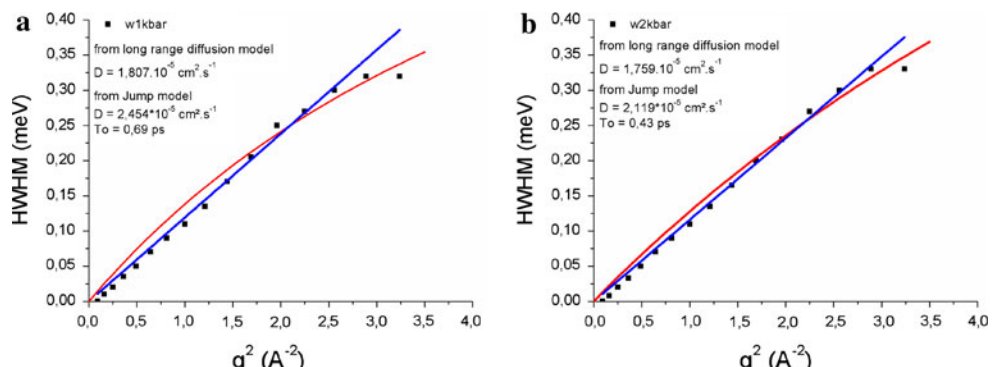


Fig. 6 q^2 Dependence of the half width at half maximum extracted from the fit of the dynamic structure factor with a single Lorentzian for the D₂O buffer at atmospheric pressure. From the fits, diffusion coefficient and residence time were extracted

Analysis of the hemoglobin dynamics

The form factor $P(q)$ (Eq. 9) is plotted as a function of the pressure in Fig. 8, together with the form factor calculated on the basis of its crystallographic structure. The experimental data are in agreement with the calculated pattern. Indeed, the characteristic helices intercorrelation peak at $q = 0.7 \text{ \AA}^{-1}$ caused by the helical structures, which are the

Fig. 7 q^2 Dependence of the half width at half maximum extracted from the fit of the dynamic structure factor according to Eq. 6 for the D₂O buffer at 1 kbar (left) and 2 kbar (right), respectively. Diffusion coefficient and residence time extracted from the fits are also shown



main secondary structures in hemoglobin protein, can be clearly seen.

The global intensity increases when applying pressure from atmospheric pressure to 2 kbar, reflecting the increase in the number of scatterers in the beam by applying pressure, as also observed by SANS in the same system (Loupiac et al. 2002). Besides this trivial change, the main effect of pressure is visible at low q , i.e., on a large spatial scale. The increase in the small-angle scattering indicates oligomerization or even aggregation of hemoglobin molecules. The helix correlation peak at 0.7 \AA^{-1} is not affected, its position remains constant over the range of applied pressures. In the pressure range between 1 bar and 2 kbar, the secondary structure of proteins, in particular the one of hemoglobin, is not disturbed. On the smaller scale accessible at high q values, the pressure has no visible effect.

The dynamic susceptibilities at different q values for the hemoglobin solution at atmospheric pressure are plotted in Fig. 9.

The band at low energy transfer is related to the center of mass diffusion, whereas the second one at higher energy transfer is due to both internal motions and water diffusion. The shift due to the D₂O diffusion can be seen in the high energy transfer range.

As can be seen in Fig. 10, the effect already observed for the pure buffer and described in Figs. 4, 5 is visible: one can see a shift of the elastic peak to lower frequencies

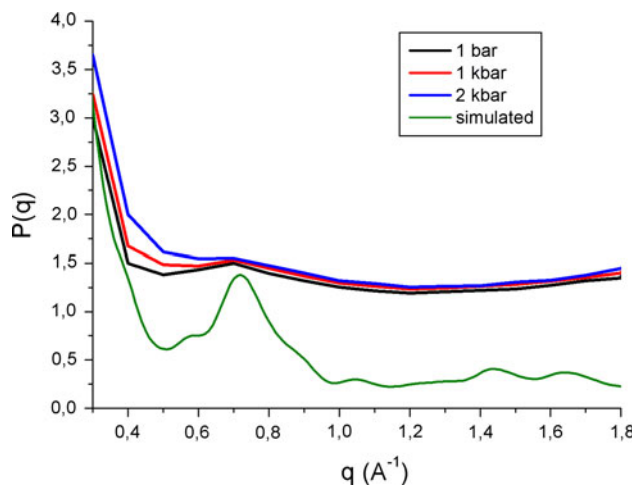


Fig. 8 Form factor of hemoglobin at atmospheric pressure, 1 and 2 kbar extracted from the fit of the dynamic structure factor with the fit function (Eq. 9), and simulated form factor of hemoglobin at atmospheric pressure, calculated from the crystallographic structure 1G08.pdb (Mueser et al. 2000)

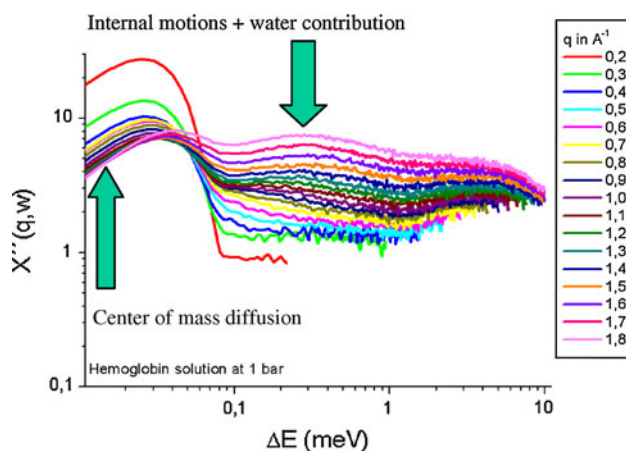


Fig. 9 q Dependence of the dynamic susceptibility for the hemoglobin solution at atmospheric pressure

as well as a shift of the quasielastic line to higher frequencies in the spectra of the protein solution. This effect is particularly apparent at high momentum transfer, but not visible any more in the pure protein signal after solvent subtraction (Fig. 11).

The susceptibility curves in Fig. 11 show that pressure up to 2 kbar has an influence on both center of mass diffusion and internal motions of hemoglobin. A shift to lower frequencies is observed, indicating a slowing down of these two processes.

The EISF, plotted in Fig. 12, is related to the ratio between the elastic amplitude and the total scattering amplitude and allows investigation of the geometry of the motion and the number of non-deuterium-exchanged

protons, essentially parts of methyl groups in side chain residues and in the protein backbone. The shape is in very good agreement with previous studies (Gaspar et al. 2008).

The EISF does not reach unity at the lowest q value, which is a sign of a small amount of multiple scattering. Nevertheless, it was found that the mean-squared displacement we would extract is still close to the true value and that the determination of the long-range diffusion is much less affected (Wuttke 2000).

One can only see a slight increase in the tail of the EISF at high q values when the pressure increases from atmospheric pressure up to 2 kbar, indicating that a small number of protons stop moving in the time window selected by the instrument resolution at these high pressure values. However, the lack of sufficiently good counting statistics makes it impossible to obtain quantitative results thus far.

The q^2 dependence of the line width of the Lorentzian L_{dif} is plotted in Fig. 13.

A linear dependence of the line width on q^2 is observed in the low- q limit. A value for the self-diffusion coefficient close to the one in literature and to the calculated one from the Stokes-Einstein theory [$D_{\text{trans}}(P = 1 \text{ bar}) = 6.50 \times 10^{-7} \text{ cm}^2 \text{ s}^{-1}$] is recovered. The effect of pressure is obvious at 2 kbar rather than at 1 kbar; a translational diffusion coefficient of $D_{\text{trans}}(P = 2 \text{ kbar}) = 5.48 \times 10^{-7} \text{ cm}^2 \text{ s}^{-1}$ has been found: the self-diffusion coefficient decreases.

On the one hand, increasing pressure induces a decrease in the hydrodynamic radius of the protein, assuming that it still exists as a tetramer. Therefore, according to the Stokes-Einstein relation, the self-diffusion coefficient is expected to increase. On the other hand, increasing pressure induces a decrease in the global protein diffusion through the increase in the solvent viscosity (Bett and Cappi 1965). Moreover, the increase in the apparent protein concentration by applying pressure may lead to a larger “cage effect,” which would also lower the global diffusion. Indeed, at 320 mg/ml, the calculated intermolecular distance would vary only from 68.7 Å at atmospheric pressure to 67.2 Å at 2 kbar. Even if this distance is larger than $2R_g$, it is smaller than $2R_H$, thus friction becomes more important at the protein hydration shell level.

We suggest interpreting the decrease in the diffusion coefficient as follows: According to the Stokes-Einstein relation, taking into account the variation in the solvent viscosity at the respective pressure values, the hydrodynamic radius was calculated to range between 34.8 Å at atmospheric pressure and 39.0 Å at 2 kbar. This could be due to an oligomerization phenomenon, which has been already observed on myoglobin under pressure (Doster et al. 2003). Considering the protein as a sphere with the

Fig. 10 Dynamic susceptibilities at $q = 0.6 \text{ \AA}^{-1}$ (left) and at $q = 1.8 \text{ \AA}^{-1}$ (right) for the hemoglobin solution at atmospheric pressure (red line), at 1 kbar (green line), and at 2 kbar (blue line)

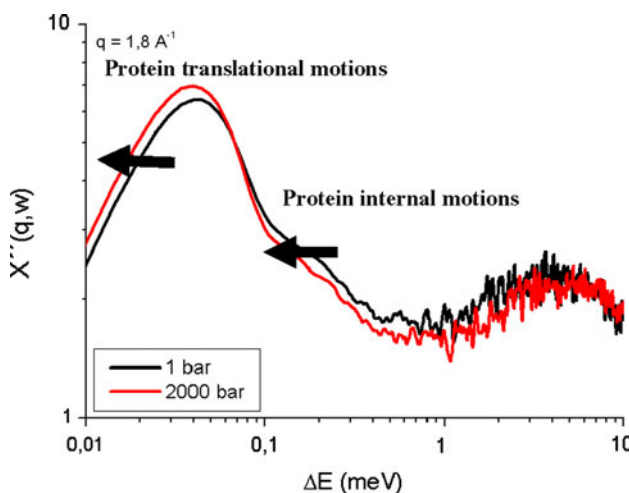
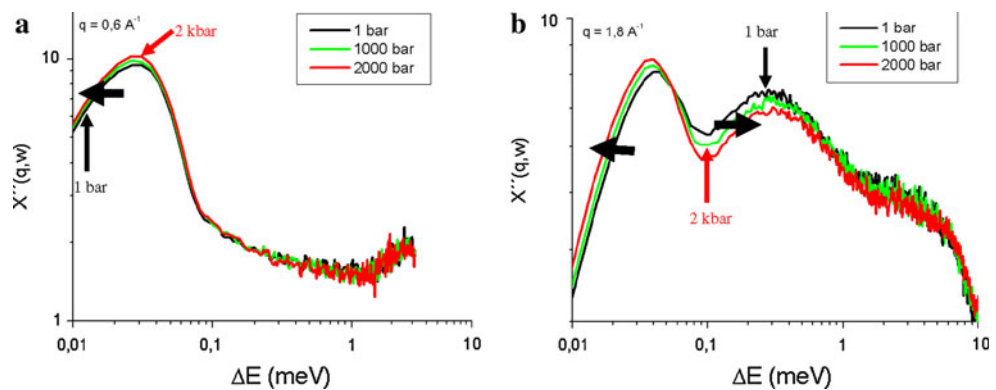


Fig. 11 Dynamic susceptibilities at $q = 1.8 \text{ \AA}^{-1}$ for the hemoglobin at atmospheric pressure (red line), at 1 kbar (green line), and at 2 kbar (blue line)

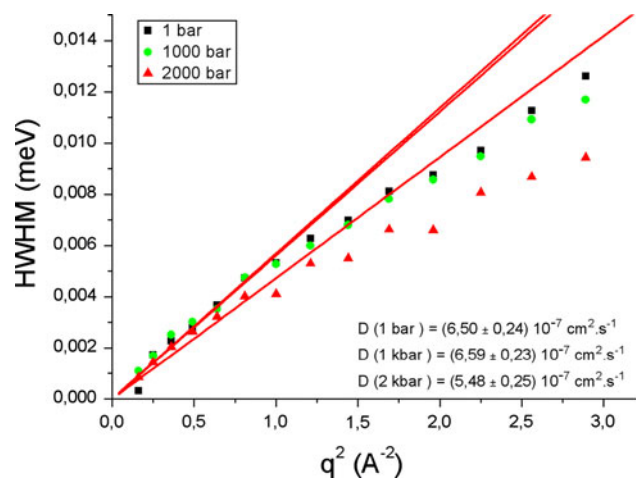


Fig. 13 Half width at half maximum of the first Lorentzian L_{dif} extracted from the fit (Eq. 9) of the dynamic structure factor of hemoglobin at atmospheric pressure, 1 and 2 kbar

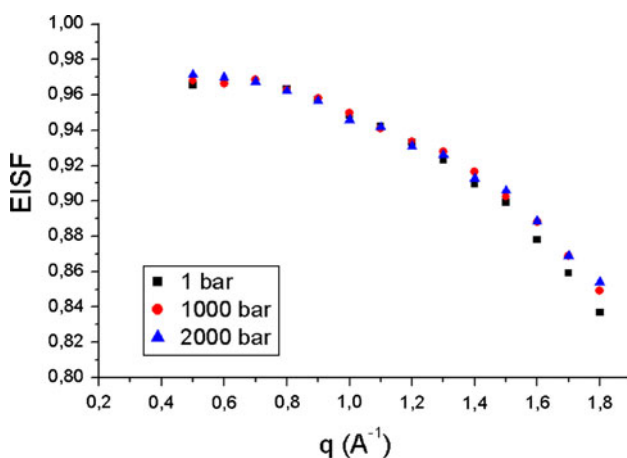


Fig. 12 Elastic incoherent structure factor of hemoglobin at atmospheric pressure, 1 and 2 kbar extracted from the fit of the dynamic structure factor with the fit function (Eq. 9)

radius of gyration $R_g = \sqrt{3/5}R_H$, the increase in volume corresponds to an increase from 4 subunits at atmospheric pressure to 5.6 subunits at 2 kbar, i.e., a distribution of

pentamers and hexamers. A gel formation was observed that has already been observed by gel strength measurements (van Camp 1996).

The q^2 dependence of the line width of the second Lorentzian L_{int} is plotted in Fig. 14.

The line width of the Lorentzian related to the relaxation time of internal motions remains constant as a function of q^2 showing the characteristic feature of local confined motions (Fig. 14). By evaluating the relaxation time from the average value of the half width at different pressures, an increase from 3.36 ps at atmospheric pressure up to 3.71 ps at 2 kbar is seen. This can be due to an increase in the density of the hydration shell of hemoglobin inducing more constraints to the motions of the lateral chain residues at the surface of the protein (Appavou et al. 2006).

Conclusions

A new aluminum 2 kbar pressure cell was built that is suitable for dynamic neutron-scattering studies on proteins

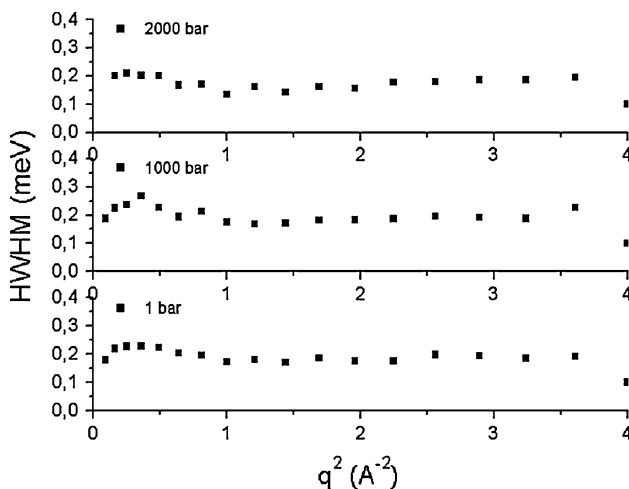


Fig. 14 Half width at half maximum of the second Lorentzian L_{int} extracted from the fit of the dynamic structure factor of hemoglobin at atmospheric pressure, 1 and 2 kbar with the fitting function (Eq. 8)

in solution as a function of pressure up to 2 kbar, featuring high transmission and low scattering power.

From quasielastic neutron-scattering experiments on a concentrated solution of hemoglobin (4.37 mM), the evaluation of the dynamic susceptibilities allowed the effect of pressure on the water dynamics to be differentiated from its effect on the protein dynamics.

The dynamics of D_2O was evaluated with a jump model. Increasing pressure led to a decrease in the diffusion coefficient and a decrease in the residence time. The latter can partially be explained by the shift of the characteristic correlation peak of D_2O in the structure factor around 2 Å^{-1} and also by hydrogen-bond rearrangement already observed by NMR (Prielmeier et al. 1987).

Both the global and internal motions of hemoglobin were slowed down by increased pressure.

A slowing down of global diffusion of the protein in solution was proposed to be due to the oligomerization of several hemoglobin subunits and to the increase in the solvent viscosity. A volume ratio calculation of the protein under pressure and atmospheric pressure yields 5.6 subunits for hemoglobin at 2 kbar, meaning that there could be a distribution between hemoglobin pentamers and hexamers. This will be tested by small-angle neutron-scattering experiments under the same conditions. The effect of pressure on the global diffusion was not reversible. In fact, a gel has been formed after pressurization, an effect that has already been observed previously by gel strength measurements.

The pressure has less effect on the extent of the internal motions but leads to an increase in their relaxation time. This can be due to the rearrangement of water molecules in the hydration shell of the protein leading to more geometrical constraints for the motions of lateral chain residues.

Acknowledgments The research project was supported by a grant of the Deutsche Forschungsgemeinschaft, SFB 533, TP B11, which is gratefully acknowledged. We would like to acknowledge particularly Joachim Dörbecker and Reinhold Funer who helped to build the 2 kbar pressure cell and the platform for TOFTOF. We would like to thank Jandal Ringe for his help on TOFTOF during our experiments. The ANTARES team, especially Martin Mühlbauer and Elbio Calzada, are thanked for allowing us to use some beam time for neutronography measurements, and to Robert Georgii for beamtime on MIRA to perform the SANS characterization measurements. Finally, we would like to thank Alan Soper for useful discussions.

References

- Appavou M-S, Gibrat G, Bellissent-Funel M-C (2006) Influence of pressure on structure and dynamics of bovine pancreatic trypsin inhibitor (BPTI): small angle and quasi-elastic neutron scattering studies. *Biochim Biophys Acta* 1764:414–423. doi:[10.1016/j.bbapap.2006.01.010](https://doi.org/10.1016/j.bbapap.2006.01.010)
- Balny C, Masson P, Heremans K (2002) High pressure effects on biological macromolecules: from structural changes to alteration of cellular processes. *Biochim Biophys Acta* 1595:3–10
- Bée M (1988) Quasi-elastic neutron scattering, principles and applications in solid state chemistry, biology and materials science. Adam Hilger, Bristol
- Bett KE, Cappi JB (1965) Effect of pressure on the viscosity of water. *Nature* 207:620. doi:[10.1038/207620a0](https://doi.org/10.1038/207620a0)
- Cavatorta F, Deriu A, Di Cola D, Middendorf HD (1994) Diffusive properties of water studied by incoherent quasi-elastic neutron scattering. *J Phys Condens Matter* 6:A113–A117. doi:[10.1088/0953-8984/6/23A/013](https://doi.org/10.1088/0953-8984/6/23A/013)
- Chen SH, Teixeira J, Nicklow R (1982) Incoherent quasielastic neutron scattering from water in supercooled regime. *Phys Rev A* 26:3477–3482. doi:[10.1103/PhysRevA.26.3477](https://doi.org/10.1103/PhysRevA.26.3477)
- Cunsolo, Orechini A, Petrillo C, RSacchetti F (2006) Quasielastic neutron scattering investigation of the pressure dependence of molecular motions in liquid water. *J Chem Phys* 124:084503. doi:[10.1063/1.2174007](https://doi.org/10.1063/1.2174007)
- Dewhurst CD (2001) GRASansP: graphical reduction and analysis SANS program. <http://www.ill.eu/lss/grasp/>
- Di Bari M, Deriu A, Filabozzi A, Andreani C, Di Venere A, Rosato N (2000) Dynamics of trypsin under pressure. *Physica B* 276–278:510–511. doi:[10.1016/S0921-4526\(99\)01831-1](https://doi.org/10.1016/S0921-4526(99)01831-1)
- Doster W, Gebhardt W (2003) High pressure—unfolding of myoglobin studied by dynamic neutron scattering. *Chem Phys* 292:383–389. doi:[10.1016/S0301-0104\(03\)00064-8](https://doi.org/10.1016/S0301-0104(03)00064-8)
- Doster W, Gebhardt R, Soper A (2003) Pressure induced unfolding of myoglobin: neutron diffraction and dynamic scattering experiments. In: Winter R (ed) Advances in high pressure bioscience and biotechnology II. Springer, Berlin, 29–33
- Edelstein SJ, Rehmar MJ, Olson JS, Gibson QH (1970) Functional aspects of the subunits association-dissociation equilibria of hemoglobin. *J Biol Chem* 245:4372–4381
- Feijoo SC, Hayes WW, Watson CE, Martin JH (1997) Effects of microfluidizer technology on *Bacillus licheniformis* spores in ice cream mix. *J Dairy Sci* 80:2184–2187. doi:[10.3168/jds.S0022-0302\(97\)76166-6](https://doi.org/10.3168/jds.S0022-0302(97)76166-6)
- Gaspar AM (2007) Methods for analytically estimating the resolution and intensity of neutron time-of-flight spectrometers. The case of the TOFTOF spectrometer. arXiv:0710.5319v1
- Gaspar AM, Appavou M-S, Busch S, Unruh T, Doster W (2008) Dynamics of well-folded and natively disordered proteins in solution: a time-of-flight neutron scattering study. *Eur Biophys J* 37:573–582. doi:[10.1007/s00249-008-0266-3](https://doi.org/10.1007/s00249-008-0266-3)

- Georgii R, Böni P, Janoschek M, Schanzer C, Valloppilly S (2007) MIRA—a flexible instrument for VCN. *Physica B* 397:150–152. doi:[10.1016/j.physb.2007.02.088](https://doi.org/10.1016/j.physb.2007.02.088)
- Longeville S, Lechner RE (2000) Light and heavy water dynamics. *Physica B* 276–278:534–535. doi:[10.1016/S0921-4526\(99\)01818-9](https://doi.org/10.1016/S0921-4526(99)01818-9)
- Loupia C, Bonetti M, Pin S, Calmettes P (2002) High-pressure effects on horse heart metmyoglobin studied by small-angle neutron scattering. *Eur J Biochem* 269:4731–4737. doi:[10.1046/j.1432-1033.2002.03126.x](https://doi.org/10.1046/j.1432-1033.2002.03126.x)
- Masson P, Tonello C, Balny C (2001) High-pressure biotechnology in medicine and pharmaceutical science. *J Biomed Biotech* 1:85–88
- McCammon JA, Harvey SC (1988) Dynamics of proteins and nucleic acids. Cambridge University Press, Cambridge
- Mueser TC, Rogers PH, Arnone A (2000) Interface sliding as illustrated by the multiple quaternary structures of liganded hemoglobin. *Biochemistry* 39:15353–15364
- Perez J, Zanotti J-M, Durand D (1999) Evolution of the internal dynamics of two globular proteins from dry powder to solution. *Biophys J* 77:454–469. doi:[10.1016/S0006-3495\(99\)76903-1](https://doi.org/10.1016/S0006-3495(99)76903-1)
- Philo JS, Lary JW, Schuster TM (1988) Quaternary interactions in hemoglobin beta-subunit tetramers. Kinetics of ligand biding and self-assembly. *J Biol Chem* 263:682–689
- Pin S, Royer CA, Gratton E, Alpert B, Weber G (1990) Subunit interactions in hemoglobin probed by fluorescence and high-pressure techniques. *Biochemistry* 29:9194–9202
- Prielmeier FX, Lang EW, Speedy RJ, Lüdemann H-D (1987) Diffusion in supercooled water to 300 MPa. *Phys Rev Lett* 59:1128–1131. doi:[10.1103/PhysRevLett.59.1128](https://doi.org/10.1103/PhysRevLett.59.1128)
- Schillinger B, Calzada E, Lorenz K (2006) Modern neutron imaging: radiography, tomography, dynamic and phase contrast imaging with neutrons. *Solid State Phenom* 112:61–71. doi:[10.4028/www.scientific.net/SSP.112.61](https://doi.org/10.4028/www.scientific.net/SSP.112.61)
- Unruh T, Neuhaus J, Petry W (2007) The high-resolution time-of-flight spectrometer TOFTOF. *Nucl Instr Meth Phys Res A* 580:1414–1422. doi:[10.1016/j.nima.2007.07.015](https://doi.org/10.1016/j.nima.2007.07.015)
- Unruh T, Neuhaus J, Petry W (2008) Erratum to “The high-resolution time-of-flight spectrometer TOFTOF”. *Nucl Instr Meth Phys Res A* 585: 201. doi:[10.1016/j.nima.2007.11.019](https://doi.org/10.1016/j.nima.2007.11.019)
- van Camp J, Huyghebaert A (1996) High pressure induced gel formation of haemoglobin and whey proteins at elevated temperatures. *Lebensm Wiss Technol* 29:49–57. doi:[10.1006/fstl.1996.0007](https://doi.org/10.1006/fstl.1996.0007)
- Wuttke J (2000) Multiple-scattering effects on smooth neutron-scattering spectra. *Phys Rev E* 62:6531. doi:[10.1103/PhysRevE.62.6531](https://doi.org/10.1103/PhysRevE.62.6531)
- Wuttke J, Ohl M, Goldammer M, Roth S, Schneider U, Lunkenheimer P, Kahn R, Rufflé B, Lechner R, Berg MA (2000) Propylene carbonate reexamined: mode-coupling beta scaling without factorization? *Phys Rev E* 61:2730–2740. doi:[10.1103/PhysRevE.61.2730](https://doi.org/10.1103/PhysRevE.61.2730)